Dynamics and asymptotical behavior of spreading processes in a closed system

Shi-Jie Xiong
Department of Physics, Nanjing University, Nanjing 210093, China
(Received 11 December 2003; published 1 June 2004)

We construct differential-integrative equations to investigate the effects of different distributions for the incubation period, defined as the period between receiving of the message and the beginning of the active state, and for the active period, the length of the active state, on the spreading dynamics in a closed system where one member can be dynamically linked to any other with given probability. The evolution of the ensemble-averaged infected rate $\gamma(t)$ is calculated by solving the equations for various distribution functions. Both the short-term oscillations and long-term saturation crucially depend on the form and parameters of the distribution functions. The obtained results may provide insights into the characteristics of oscillations and a prognosis of a spreading process in closed system.

DOI: 10.1103/PhysRevE.69.066102 PACS number(s): 89.75.Fb, 87.23.Ge, 05.70.Fh, 05.70.Ln

I. INTRODUCTION

In spite of the complexity of networks in the real world, such as the Internet [1], the food webs [2], the spreading webs of epidemic diseases [3], and the scientific collaboration networks [4], their basic and common statistical characteristics seem to be well described and simulated with exceedingly simple models, and have attracted extensive interest among physicists. In this context knowledge of the building of statistical models, of ensemble theories, and of methods developed for the study of phase transitions and cooperative phenomena in many-body systems becomes helpful in the understanding of the real-world networks which are outside the traditional realm of physics. In these efforts models based on small-world networks (SWN's), introduced by Watts and Strogatz [5], have been intensively investigated. A SWN is made of a lattice in a d-dimensional space in which a fraction (p) of bonds are replaced with new bonds linking to sites randomly distributed on the lattice. As the new bonds can connect sites very far away in space, they make a big world become a small one. This effect is quantitatively described by the averaged shortest distance between any two sites, $\overline{l}$, which follows the scaling law $\overline{l}(N,p) \sim (N^*)^{1/d} F(N/N^*)$ with $F(u)$ having limits $F(u) \sim u^{1/d}$ for $u \ll 1$, $F(u) \sim \ln u$ for $u \gg 1$, and $N^* \sim p^{-1}$ being a crossover size separating the big- and small-world regimes [6,7]. It is also shown that in the quantum version of SWN's the electron states are more likely to be extended among the whole system, in spite of the localization effect of the randomness [8]. Recently, it is shown that a nonequilibrium phase transition can occur in directed small-world networks [9].

Our life is intimately connected with spreading processes in social, biological, and economic systems. As common features, every process is constituted with many subprocesses of the transmission of a specific "message" from one individual to another, and the whole process is non-Markovian and irreversible. Recently, effects of heterogeneity and topology in networks on the dynamics of spreading have attracted much attention of researchers. There are two types of networks: the exponential networks, such as the random graph model [10] and the SWN [5], in which the nodes' connectivity is exponentially bounded, and the so-called scale-free (SF) networks that exhibit a power-law connectivity distribution [11–13]. It is shown that a susceptible-infected-susceptible (SIS) model on SF networks has no epidemic threshold [13], contrary to the threshold theory in epidemiology [14]. The studies of susceptible-infected-recovered (SIR) models also show the crucial role of heterogeneity in networks on the spreading [15,16]. Besides the studies of the long-term behavior such as the epidemic threshold, the short-term behavior such as the oscillatory prevalence has also been studied [17].

Although the effects of the "spatial" heterogeneity or topology of networks on the spreading dynamics have been extensively studied, studies of effects of "temporal" structures in the prevalence are still rare. In fact, for a given epidemic disease there exist characteristic distribution functions for the incubation period, defined as the period between the receiving of the message and the beginning of the active state, and for the active period, defined as the length of the active state. These distribution functions reflect the nature of the relevant virus, the level of curing, and the discrepancy in response among individuals. The temporal structure of the developing and curing of an epidemic disease can be specified by these distribution functions. Similar to the spatial topology of networks, such a temporal structure has also crucial effects on the long-term and short-term behavior of the spreading dynamics. Most previous studies of spreading dynamics, however, did not consider details of the temporal structure. For example, in the SIS and SIR models which are widely used to study the dynamics in various networks, the developing or curing process is simply characterized by a single parameter, the deactivated rate or the recovery rate. As we will see below, this single parameter corresponds to a quarter-sine-shaped distribution function. In practice, a large number of parameters are needed to specify a distribution function: its cumulants of different orders. A single parameter is not enough even for specifying the basic features of a distribution: the first and second cumulants corresponding to the mean value and the width of the distribution. In this paper we adopt differential-integrative equations to investigate the effects of distributions for the incubation and active periods on the spreading dynamics in a closed system where one member can be dynamically linked to any others with

given probability. The evolution of the ensemble-averaged infected rate $\gamma(t)$ is calculated by solving the equations for various distribution functions. It is found that both short-term oscillations and long-term saturation crucially depend on the form and parameters of these distribution functions. The results obtained reproduce oscillations with different shapes observed in many practical processes and present a quantitative dependence of the saturated infected rate on the form and parameters of the distributions and on the system size. The saturated infected rate is a crucial quantity for the prognosis estimation of a spreading process in a closed system. For example, if a disease is spreading in a biological species without control, one may be interested in the question whether all the individuals will be infected. If the saturated value of the infected rate is 1, the answer to this question is "yes" and the species may be annihilated. If it is less than 1, there will be a finite number of survivals at the end and the species will survive. As a platform we adopt a closed system in which every pair of members has a probability, denoted by c, to be linked during a unit time t_0, and all the links randomly vary with time. The spreading begins from one or more seed members, who receive the message at $t=0$. After an incubation period t_1 from receiving, they become active and begin to send out the message to other members via links. Those members receiving the message also become active after their own incubation time, and the spreading is continued. Every active member stops to send out the message after an active period t_2, reflecting the fact that an infected person will not infect others after cure or death in the epidemic spreading or a person becomes uninterested in spreading the message in the processes of information spreading. Thus, for every member there are three possible states: the unaffected state, infected but not active state of period t_1, and active state of period t_2. This is similar to the SIR models for the epidemic processes, but now two relaxation times are introduced, making the model non-Markovian and more suitable for the study of the dynamics. The results show that although the short-term behavior is sensitive to most of the parameters, there are only few parameters (mainly t_2) that have an essential effect on the long-term behavior. The spatial structure of the model corresponds to the small-world limit ($p\rightarrow 1$) of the SWN. This is a simple network so that we can focus on the effects of the temporal structure.

II. DIFFERENTIAL-INTEGRATIVE EQUATIONS

Let us construct equations governing the dynamics of the ensemble-averaged number of infected members who have received the message, $S(t)$, and the averaged number of active members, $D(t)$, in a closed system with N members. During a unit time at moment t, there are averagely $cD(t)\times[N-S(t)]$ links, each of which connects an active member and an unaffected member. Thus, the increase of infected members in this unit time can be written as

$$\frac{dS(t)}{dt} = cD(t)[N - S(t)]. \tag{1}$$

We assume that $P_1(t)$ and $P_2(t)$ are distribution functions of incubation and active periods for all members, respectively. A member who receives the message at t will become active after his incubation period. This active state will last during his active period. After that he will be permanently inactive. So the increase of the averaged active number in a unit time at moment t is

$$\frac{dD(t)}{dt} = \int_0^t dt' \left[\frac{dS(t')}{dt'} P_1(t-t') - \int_0^{t'} dt'' \frac{dS(t'')}{dt''} P_1 \times (t'-t'') P_2(t-t') \right]. \tag{2}$$

Here the integrations are used for the ensemble average. We assume that the spreading process is started at $t=0$ from some seed members. Thus, the initial conditions are

$$S(t<0) = D(t\leqslant 0) = 0, \quad S(t=0) = S_0, \tag{3}$$

where S_0 is the number of seed members. By rescaling the time, $\tau \equiv t/(cN)$, and defining infected rate $\gamma(\tau) \equiv S(\tau)/N$ and active rate $\eta(\tau) \equiv D(\tau)/N$, Eqs. (1)–(3) can be rewritten as

$$\frac{d\gamma(\tau)}{d\tau} = \eta(\tau)[1-\gamma(\tau)], \tag{4}$$

$$\frac{d\eta(\tau)}{d\tau} = \int_0^\tau d\tau' \left[\frac{d\gamma(\tau')}{d\tau'} \tilde{P}_1(\tau-\tau') - \int_0^{\tau'} d\tau'' \frac{d\gamma(\tau'')}{d\tau''} \tilde{P}_1 \times (\tau'-\tau'') \tilde{P}_2(\tau-\tau') \right], \tag{5}$$

$$\gamma(\tau<0) = \eta(\tau\leqslant 0) = 0, \quad \gamma(\tau=0) = \gamma_0 \equiv S_0/N, \tag{6}$$

where $\tilde{P}_1(\tau)$ and $\tilde{P}_2(\tau)$ are probabilities $P_1(t)$ and $P_2(t)$ expressed with rescaled time. Equations (4)–(6) are not explicitly dependent on c and N, and we can solve them and then substitute $\tau = cNt$ into the solutions to obtain the behavior of system with specific values of c and N.

III. DYNAMICS AND ASYMPTOTIC BEHAVIOR FOR DIFFERENT DISTRIBUTION FUNCTIONS OF INCUBATION AND ACTIVE PERIODS

The form and parameters of distribution functions $P_1(t)$ and $P_2(t)$ have crucial effects on the spreading dynamics. In SIS or SIR models the transition from infected to recovered (or removed) state is described by a single parameter, the average recovered (or removed) rate β. This corresponds to a distribution function $P_{\mathrm{SIR}}(t)$ for the period from infected to recovered (removed) state which satisfies equation

$$\frac{dP_{\mathrm{SIR}}(t)}{dt} = \beta\left(1 - \int_0^t P_{\mathrm{SIR}}(\tau)d\tau\right), \tag{7}$$

with initial conditions $P_{\mathrm{SIR}}(t)|_{t=0}=0$ and $dP_{\mathrm{SIR}}(t)/dt|_{t=0}=\beta$ and the constriction that $\int_0^t P_{\mathrm{SIR}}(\tau)d\tau$ cannot be greater than 1. From this one can easily see that the distribution function of the SIR or SIS models has the quarter-sine form

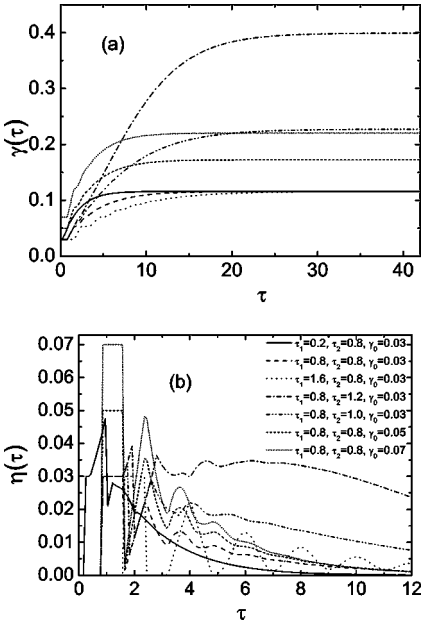

FIG. 1. Infected rate γ (a) and active rate η (b) as functions of rescaled time τ for the δ-function distribution. Parameter values are shown in panel (b).

$$P_{\mathrm{SIR}}(t) = \begin{cases} \sqrt{\beta}\sin(\sqrt{\beta}t), & \text{for} \dfrac{\pi}{2\sqrt{\beta}} \geqslant t \geqslant 0, \\ 0, & \text{otherwise}. \end{cases} \tag{8}$$

This form of distribution is not sufficient to describe the variety of the temporal structure in practice. Especially, one needs at least two parameters—the mean value and the width—to specify the basic feature of a distribution. In the following we consider different distribution functions and investigate their effects on the dynamics.

A. δ probabilities for incubation and active periods

At first we consider the δ probabilities $P_1(t)=\delta(t-t_1)$ and $P_2(t)=\delta(t-t_2)$. In this case all the members have the same incubation and active periods t_1 and t_2, and the distribution width is zero. This may provide information on the effects of the mean values of incubation and active periods. By substituting δ functions into Eqs. (4) and (5) one gets

$$\frac{d\gamma(\tau)}{d\tau} = [1-\gamma(\tau)][\gamma(\tau-\tau_1)-\gamma(\tau-\tau_2-\tau_1)], \tag{9}$$

where $\tau_{1,2}=cNt_{1,2}$. Together with the initial condition (6), there are three parameters τ_1, τ_2, and γ_0 determining the dynamics. In Fig. 1 we plot the evolution of $\gamma(\tau)$ and $\eta(\tau)$ for different values of parameters. For all parameter values the infected rate is saturated at the large-τ limit. The saturated infected rate $\gamma(\infty)$ depends on τ_2 and γ_0, but is independent of τ_1. The long-term behavior relies on the initial condition due to the non-Markovian nature of the processes. The rescaled active period τ_2 is also an important parameter determining both the short-term and long-term behavior. The rescaled incubation period τ_1 only infects the short-term behavior. For small τ, there are oscillations in η. By increasing τ_1, both the period and amplitudes of oscillations are increased. It can be seen that in some case— e.g., the dotted line— the oscillatory prevalence may be recovered from a temporary silence of almost complete extinction. Such behavior of oscillations is often observed in practice [18], but is not explained by usual statistical analysis. The present results imply that the oscillatory behavior can be attributed to the existence of the incubation period, and a recoverable prevalence after a complete silence can occur if the incubation period is long enough compared with the active period. In all cases oscillations are damped out for large τ due to the finite size of the closed system.

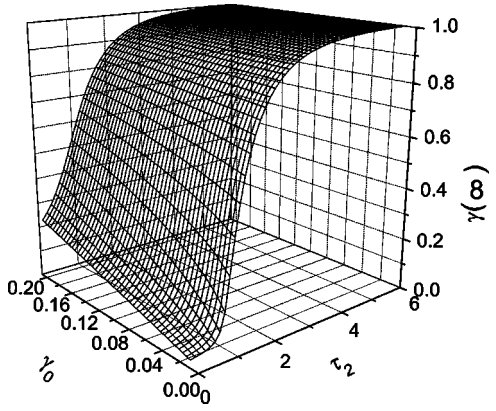

FIG. 2. Saturated infected rate $\gamma(\infty)$ as a function of rescaled active period τ_2 and initial seed rate γ_0.

In Fig. 2 we plot the dependence of the saturated infected rate $\gamma(\infty)$ on τ_2 and γ_0. It can be seen that $\gamma(\infty)$ varies from 0 to 1 by increasing τ_2 and fixing γ_0, and only slightly increases by fixing τ_2 and increasing γ_0. All the data in Fig. 2 can be fitted with the Hill function as shown in Fig. 3,

$$\gamma(\infty) \sim \frac{\tau_2'^{\mu}}{k^{\mu}+\tau_2'^{\mu}}, \tag{10}$$

where τ_2' is the active period renormalized with the initial value as $\tau_2'=\tau_2+a\gamma_0 e^{-b\tau_2}$ with $a\sim 5.1$ and $b\sim 0.96$, and the fitting parameters are $k=1.351\pm0.003$ and $\mu=3.64\pm0.03$.

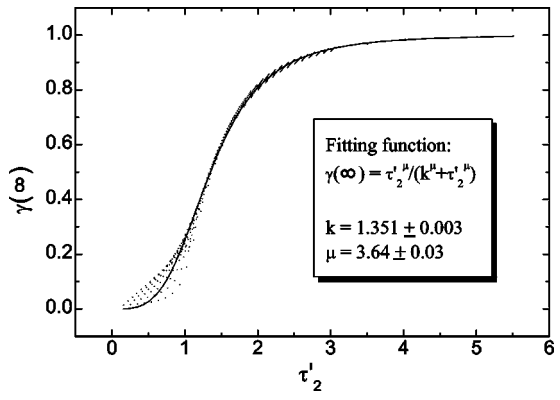

FIG. 3. Saturated infected rate $\gamma(\infty)$ as a function of renormalized active period τ_2' (dots) and the fitting function (solid line).

For a large system, the rate of initial seeds is small, $\gamma_0 \ll 1$. In this case $\tau_2' \sim \tau_2$, and the asymptotic behavior is only determined by τ_2.

The obtained results show that for a spreading process in a closed system there exists a dimensionless "risk" index $\tau_2 = cNt_2$, which determines whether the spreading can cover everyone in the system. If $\tau_2 \gtrsim 3$, all individuals in the system will be infected in a sufficiently long time, because in this case $\gamma(\infty) \sim 1$. If c and t_2 are fixed, the risk index is proportional to the size of the system. This implies that larger species with high population, such as dinosaurs, are more frangible than smaller species with low population to the spreading of epidemic diseases. Another example is the prevalence of the bird flu among chickens in a closed farm or village. For fixed c and t_2, the final survival rate of chickens in a large chicken farm is much smaller than that in a village where there are only a few chickens fed by villagers. For a given system size the risk index can be quantitatively estimated from the density of links c and the active period t_2.

B. Uniform distribution probabilities for incubation and active periods

Owing to the discrepancies among individuals, the distribution probabilities usually have finite widths. A simple form for describing widths is the uniform distribution in a window— i.e.,

$$P_{1(2)}(t) = \frac{1}{W_{1(2)}} \theta\left(t - t_{1(2)} + \frac{W_{1(2)}}{2}\right) \times \theta\left(t_{1(2)} + \frac{W_{1(2)}}{2} - t\right), \tag{11}$$

where $t_{1(2)}$ is the averaged incubation (active) period and $W_{1(2)}$ is the corresponding distribution width. With the time rescaling one has rescaled average periods $\tau_{1(2)} = cNt_{1(2)}$ and rescaled widths $w_{1(2)} = cNW_{1(2)}$. By substituting them into Eq. (5), we have

$$\frac{d\eta(\tau)}{d\tau} = \frac{1}{w_1}[\gamma(\tau_1^-) - \gamma(\tau_1^+)] - \frac{1}{w_1 w_2}\int_{\tau_2^+}^{\tau_2^-} d\tau'[\gamma(\tau_1'^-) - \gamma(\tau_1'^+)], \tag{12}$$

where $\tau_{1(2)}^{\pm} = \tau - (\tau_{1(2)} \pm w_{1,2}/2)$ and $\tau_1'^{\pm} = \tau' - (\tau_1 \pm w_1/2)$. Together with Eq. (4), one can numerically solve the evolution of $\gamma(\tau)$ and $\eta(\tau)$.

In Figs. 4(a) and 4(b) we plot the evolution of the active and infected rates for given τ_1 and τ_2 and different w_1 and w_2. It can be seen that the increase of diversity of both the incubation and active periods reduces the oscillations of the active rate, but does not change the overall trend of the evolution of $\gamma(\tau)$. Especially, the recoverable prevalence after a complete silence can still occur if the width of distribution of the incubation period is finite but small, and it will disappear if w_1 is large enough. The conclusions on the long-term behavior, such as the value of $\gamma(\infty)$, obtained for the δ-function distributions are still valid.

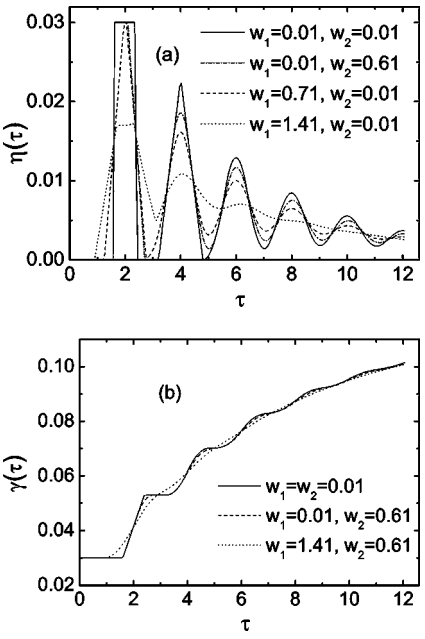

FIG. 4. Active rate η (a) and infected rate γ (b) as functions of rescaled time τ for uniform distributions with different w_1 and w_2. Other parameters are $\tau_1 = 1.6$, $\tau_2 = 0.8$, and $\gamma_0 = 0.03$.

C. Poisson distributions for incubation and active periods

The diversity widths in the uniform distributions have no effect on the long-term behavior. This may be due to the sharp drops at the edges. The situation could be changed if the distributions have long-term tails. Here we consider the Poisson distribution which is written as

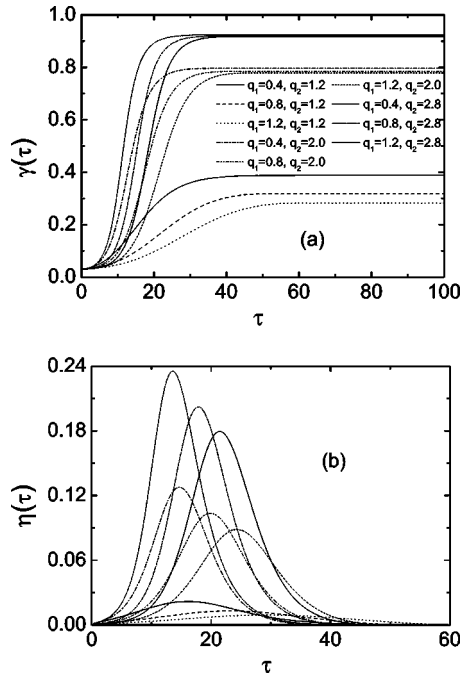

FIG. 5. Infected rate γ (a) and active rate η (b) as functions of rescaled time τ for the Poisson distribution. $\gamma_0 = 0.03$, and other parameters are shown in panel (a).

$$\tilde{P}_{1(2)}(\tau) = \frac{1}{q_{1(2)}} e^{-\tau/q_{1(2)}}, \tag{13}$$

where $q_{1(2)}$ is a parameter characterizing the rescaled average incubation (active) period. By substituting Eq. (13) into Eqs. (4) and (5) and numerically solving them, we obtain the evolution of the infected and active rates. The results for various values of q_1 and q_2 are shown in Fig. 5. From Fig. 5(a) we see that $\gamma(\tau)$ still saturates to a value less than 1 and the saturated value increases with q_2. Differently from δ-function and uniform distributions, now $\gamma(\infty)$ not only depends on q_2, but also decreases with increasing q_1. The q_1 dependence of $\gamma(\infty)$ decreases when q_2 increases. This dependence is due to the long tail of the τ_1 distribution for which the long-term rate of the receiving-but-not-active individuals can reduce the rate of new receivers. In Fig. 5(b) there are no oscillations in $\eta(\tau)$ for any q_1 and q_2, owing to the wide nature of the Poisson distribution. The evolution curves of $\eta(\tau)$ follow a Gaussian-like behavior, similar to many realistic curves of epidemic spreading processes without oscillations.

IV. CONCLUSIONS

As a summary, from simulations of spreading processes in a closed system at the small-world limit with different types of distribution functions for the incubation and active periods, it is found that the final infected rate of the spreading is mainly determined by a dimensionless risk index τ_2, proportional to the system size, contact density, and average active period. When τ_2 is larger than a critical value of 3, the final infected rate can reach unity, implying coverage of the spreading over the whole system. The final infected rate is only slightly affected by the initial seed rate due to the non-Markovian nature. In the case of Poisson distributions it is also slightly affected by the incubation period. In many cases with finite incubation period the short-term behavior shows oscillations. The shape and amplitude of oscillations depend on both distributions of the incubation and active periods. The amplitude of oscillations is reduced by increasing the widths of the distributions. If the incubation period is long enough and the distribution width is small, a recoverable prevalence after a complete silence can occur. The results quantitatively show the crucial effects of the temporal characteristics on both the long-term and short-term behavior of the spreading dynamics.

ACKNOWLEDGMENTS

This work was supported by National Foundation of Natural Science in China Grant No. 60276005 and by the China State Key Projects of Basic Research Grant No. (G1999064509).

[1] B. A. Huberman and L. A. Adamic, Nature (London) **401**, 131 (1999); R. Albert, H. Jeong, and A.-L. Barabási, *ibid.* **401**, 130 (1999).
[2] S. L. Pimm, J. H. Lawton, and J. E. Cohen, Nature (London) **350**, 669 (1991); R. T. Paine, *ibid.* **355**, 73 (1992); K. McCann, A. Hastings, and G. R. Huxel, *ibid.* **395**, 794 (1998).
[3] C. Moore and M. E. J. Newman, Phys. Rev. E **61**, 5678 (2000); M. Kuperman and G. Abramson, Phys. Rev. Lett. **86**, 2909 (2001); M. E. J. Newman, Phys. Rev. E **66**, 016128 (2002).
[4] M. E. J. Newman, Proc. Natl. Acad. Sci. U.S.A. **98**, 404 (2001).
[5] D. J. Watts and S. H. Strogatz, Nature (London) **393**, 440 (1998).
[6] Reka Albert and Albert-Laszlo Barabási, Rev. Mod. Phys. **74**, 47 (2002), and references therein.
[7] S. N. Dorogrovtsev and J. F. F. Mendels, Adv. Phys. **51**, 1079 (2002), and references therein.
[8] Chen-Ping Zhu and Shi-Jie Xiong, Phys. Rev. B **62**, 14 780 (2000); **63**, 193405 (2001).
[9] A. D. Sánchez, J. M. López, and M. A. Rodríguez, Phys. Rev. Lett. **88**, 048701 (2002).
[10] P. Erdös and P. Rényi, Publ. Math. Inst. Hung. Acad. Sci. **5**, 17 (1960).
[11] A.-L. Barabäsi and R. Albert, Science **286**, 509 (1999).
[12] A.-L. Barabäsi, R. Albert, and H. Jeong, Physica A **272**, 173 (1999).
[13] R. Pastor-Satorras and A. Vespignani, Phys. Rev. E **63**, 066117 (2001).
[14] N. Shigesada and K. Kawasaki, *Biological Invasions: Theory and Practice* (Oxford University Press, Oxford, 1997).
[15] R. M. May and A. L. Lloyd, Phys. Rev. E **64**, 066112 (2001).
[16] M. E. J. Newman, Phys. Rev. E **66**, 016128 (2002).
[17] Y. Hayashi, M. Minoura, and J. Matsukubo, Phys. Rev. E **69**, 016112 (2004).
[18] J. O. Kephart and S. R. White, in *Proceedings of the 1993 IEEE Computer Society Symposium on Research in Security and Privacy*, sponsored by the IEEE Computer Society, Technical Committee on Security and Privacy in cooperation with the International Association for Cryptologic Research (IACR) (IEEE, Washington, D. C., 1993), p. 2.